A spatiotemporally resolved GPCR interactome reveals novel mediators of receptor agonism

Authors: Maria M. Shchepinova,[1,*] Rachel Richardson,[2] Jack W. Houghton,[1] Abigail R. Walker,[2] Daniel Conole,[1§] Aylin C. Hanyaloglu,[2,*] Edward W. Tate[1,*]

Affiliations:

[1]Department of Chemistry, Molecular Sciences Research Hub, Imperial College London, 82 Wood Lane, London W12 0BZ, UK

[2]Institute of Reproductive and Developmental Biology (IRDB), Department of Metabolism, Digestion and Reproduction, Imperial College London, Hammersmith Campus, Du Cane Road, London W12 0NN, UK.

[§]Present address: Auckland Cancer Society Research Centre, Faculty of Medical and Health Sciences, University of Auckland, 85 Park Road, Grafton, Auckland 1023, New Zealand

*Corresponding authors. E-mails: m.shchepinova@imperial.ac.uk; a.hanyaloglu@imperial.ac.uk; e.tate@imperial.ac.uk

Summary

Cellular signaling by membrane G protein-coupled receptors (GPCRs) is orchestrated by a complex and diverse array of mechanisms. The dynamics of a GPCR interactome as it evolves over time and space in response to an agonist can offer a unique window on pleiotropic signaling decoding and functional selectivity at a cellular level. In this study, we employed proximity-based APEX2 proteomics to interrogate the interaction network of the GPCR for luteinizing hormone (LHR) on a sub-minute timescale. We developed an analytical approach integrating quantitative multiplexed proteomics and temporal reference profiles, providing a platform to identify the proteomic environment of APEX2-tagged LHR at the nanometer scale. LHR activity is exquisitely regulated at a spatial level, leading to identification of novel interactors including the Ras-related GTPase RAP2B that modulate both receptor signaling and post-endocytic trafficking, and providing a resource for spatiotemporal nanodomain mapping of LHR interactors across subcellular compartments.

Introduction

The G protein-coupled receptor (GPCR) superfamily plays a central role in cellular communication and signaling [1-3]. Current models of GPCR signaling have evolved beyond a single GPCR activating a specific heterotrimeric G protein pathway at the cell surface to encompass dynamic multidimensional signaling hubs [4]. These include the ability of GPCRs to activate multiple G proteins, associate with an array of adaptor proteins [5] and form oligomeric complexes [6,7]. Furthermore, GPCRs assemble distinct signaling hubs in varied subcellular compartments in addition to the plasma membrane, including endosomes [8], the nucleus [9], Golgi and mitochondria [4,10]. Collectively, this kaleidoscopic diversity of mechanisms offers multiple layers to regulate functional selectivity for a specific GPCR ligand [4]. To understand the relevance of GPCR signaling in health and disease, we must develop methods to understand how such complexity is decoded by cells to direct downstream functions.

The luteinizing hormone receptor (LHR) is an example of a GPCR that exhibits cell signaling pleiotropy (the ability of the receptor to produce several different signaling outputs in response to ligand binding). This pleiotropy is thought to mediate its diverse roles in reproduction and pregnancy, harnessing poorly understood mechanisms to regulate signaling activated by its endogenous ligand luteinizing hormone (LH) at a spatiotemporal level (**Figure 1A**) [11-13]. Whilst LHR is primarily coupled to the heterotrimeric G protein $G_{\alpha}s$, thereby increasing levels of the second messenger cyclic AMP (cAMP), under conditions of high LHR expression and/or LH levels observed in ovaries, it may also activate $G_{\alpha}q/11$ signaling pathways, leading to activation of phospholipase C-β (PLC-β) [14-16]. Activated LHR also robustly recruits canonical GPCR adaptor proteins β-arrestin-1 and -2 for rapid G protein desensitization, internalization from the plasma membrane to endosomes and activation of additional signaling pathways, such as mitogen activated protein kinases (MAPKs) [12,17,18]. Indeed, the location or spatial control of LHR is critical for shaping LHR activity, whereby receptor internalization is essential for its acute $G_{\alpha}s$-cAMP signaling [19]. The LHR initiates this G protein signaling via receptor internalization and trafficking to a unique endosomal compartment termed the very early endosome (VEE), which plays a key role in sorting receptors to post-endocytic trafficking pathways (**Figure 1A**) [19,20]. In contrast to the early endosome, the VEE is of smaller size, and lacks classical early endosomal markers such as EEA1, phosphatidylinositol 3-phosphate (PI3P) and Rab5 [20]. LHR is a paradigm example of a GPCR regulated by the VEE, which is a platform for acute intracellular G protein signaling, sustained MAPK signaling mediated by interactions with the PDZ domain protein GIPC1 ($G_{\alpha}i$-interacting protein C-terminus 1) during ligand-induced endocytosis, and rapid recycling to the plasma membrane, driven by the protein APPL1 (Adaptor protein containing PH domain, PTB domain and Leucine zipper motif), which also functions in the VEE to negatively regulate LHR G protein signaling via distinct mechanisms [19,21]. APPL1, the only adaptor protein previously shown to localize to VEE, marks only a subpopulation of LHR-containing VEEs [19], and

the protein machinery driving LHR activity through these critical sorting and signaling compartments remain poorly understood.

Proximity labeling-enabled proteomics of interacting proteins (interactomics) is an emerging and powerful approach to interrogate protein interaction networks at both the spatial and temporal level, directly in intact cells [22-27]. The approach applies proximity-based biotinylation through a fusion of the protein of interest with APEX2, an engineered ascorbate peroxidase domain [28], coupled to enrichment and quantitative mass spectrometry proteomics. APEX2 proximity proteomics was first applied to GPCRs to identify known and novel interactors of β_2-adrenergic receptor [29,30], angiotensin II type 1 receptor [29], δ-opioid receptor [30] and μ-opioid receptor [31]. Rapid labeling within 30 seconds over a distance of up to 20 nm from the GPCR-APEX2 fusion offers a particular advantage for the analysis of GPCR signaling interactome, where receptor activation, internalization and recycling typically occurs on a timeframe of seconds to minutes [32]. Here, we employed LHR-APEX2 fusions to interrogate the ligand-induced LHR interaction network, with sub-minute temporal resolution. Harnessing known time-dependent LHR-protein associations through a multi-layered quantitative interactome analysis pipeline, we established the first approach to spatiotemporally identify and characterize the LHR interactome during receptor activation in intact cells and identify multiple novel LHR interactors which direct very early endosomal sorting and signaling. Taken together, this study provides a roadmap for analysis and functional interrogation of receptor-mediated quantitative proximity labeling proteomics datasets.

Results

Establishing an LHR-APEX proximity labeling platform. To validate our system, we set out to apply an LHR proximity labeling platform (**Figure 1B**) to identify the LH (agonist)-dependent LHR interactome over a 1-10 minute time window (**Figure 1C**), with the aim to capture well-established key steps in receptor signal activation, internalization, and subsequent trafficking, based on the current knowledge of LHR activity profiles (**Figure 1A**) [19,20]. We stably expressed LHR C-terminally tagged with APEX2 [28] in tetracycline-inducible Flp-In T-REx 293 cells [33] (**Figure S1A**), and went on to confirm that this novel fusion preserved the expected expression, internalization and recycling behavior of LHR [19,20]. LHR-APEX2 exhibited plasma membrane expression and LH-induced internalization to small endosomes characteristic of VEEs, in a manner identical to cells stably expressing N-terminally tagged FLAG-LHR without APEX2 fusion (**Figure 1D**), and it also recycled to the plasma membrane (**Figure S1B**). The ability of LHR-APEX2 to activate G_{α}s-cAMP was also compared to FLAG-LHR expressing cells, and both cell lines were found to produce similar LH-mediated cAMP dose-response curves with comparable values for half maximal effect concentration (EC_{50}) and maximum response (E_{max}) (**Figure 1E**). Cells without tetracycline treatment did not show

detectable LHR activity upon activation with LH (**Figure 1E**). Taken together, these results indicate that C-terminal APEX2 tagging did not impair protein interactions required for recycling or activation of key G protein signal pathways, and the key elements of the interactome are preserved.

To optimize the proximity labeling reaction (**Figure 1B**), Flp-In T-REx LHR-APEX2 cells were induced with tetracycline overnight, and then pre-incubated in biotin-phenol for 30 min followed by stimulation with the agonist LH for either 1, 2, 3, 5 or 10 min (**Figure 1F**). Each sample was treated with hydrogen peroxide for 60 seconds to initiate APEX2-catalyzed proximity biotinylation, followed by immediate quenching with ice-cold quenching buffer. For controls, “no hydrogen peroxide” or “no agonist” treatments were used, as in previous APEX studies [29,30,34-36].

Cells were harvested, lysed, and proteins precipitated. The levels of streptavidin-HRP, as measured by western blotting, demonstrated strong biotinylation present in all samples apart from controls lacking hydrogen peroxide treatment (**Figure 1G**), which revealed only endogenous biotinylated carboxylases at ca. 75 and 130 kDa, as expected [34,37]. These biotinylated proteins could be successfully pulled-down on streptavidin-coated agarose beads (**Figure S1C**).

For subsequent proteomic analyses (**Figure 1F**), “no hydrogen peroxide” and “no agonist treatment” controls were used, and proximity labeling was carried out in three independent replicates.

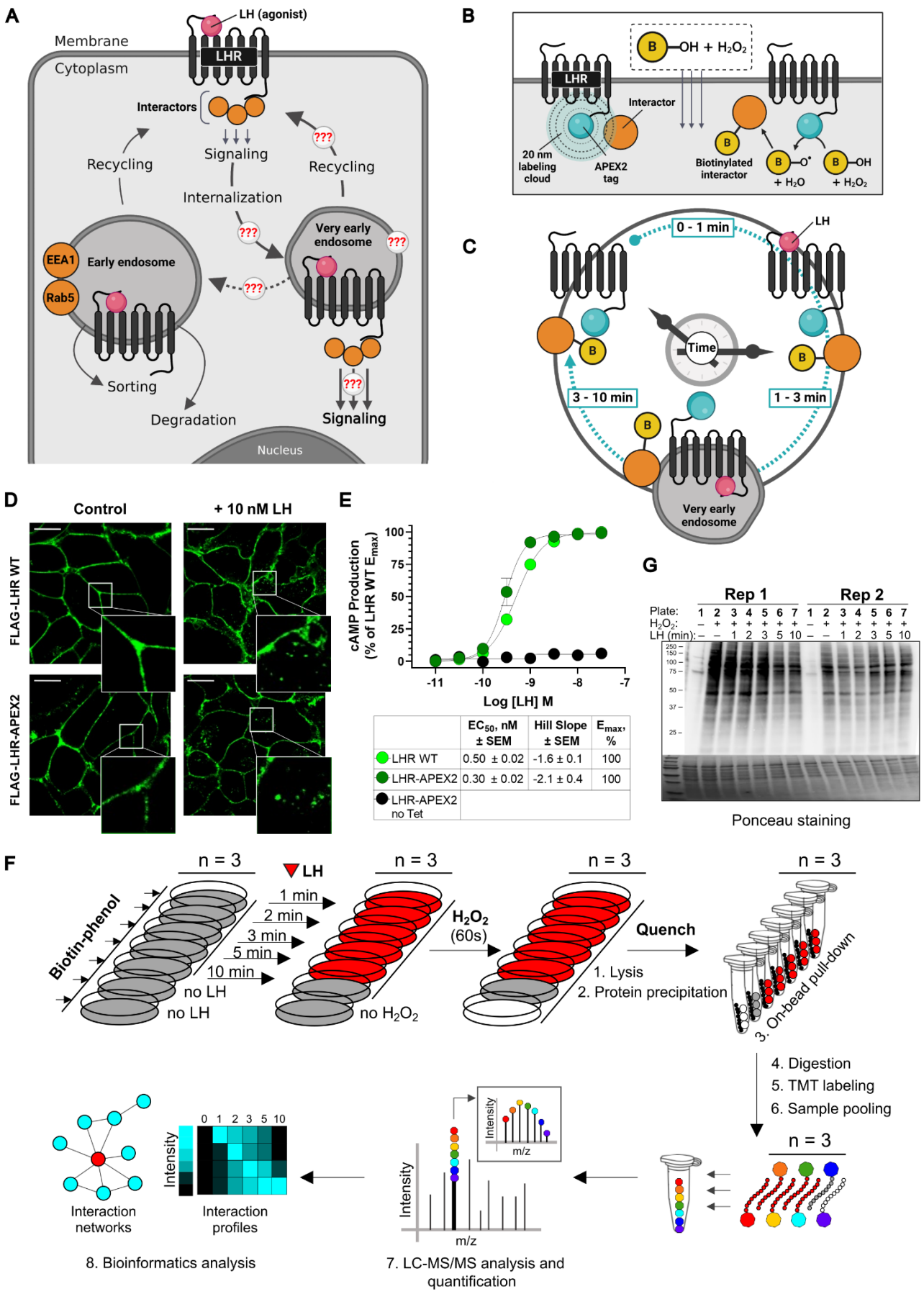
A
LH (agonist)
Membrane
Cytoplasm
LHR
Interactors
Signaling
Recycling
Recycling
Internalization
Very early endosome
EEA1
Early endosome
Rab5
Sorting
Degradation
Signaling
Nucleus
B
B—OH + H2O2
LHR
Interactor
20 nm labeling cloud
APEX2 tag
Biotinylated interactor
+ H2O
+ H2O2
C
0 - 1 min
LH
Time
3 - 10 min
1 - 3 min
Very early endosome
D
Control
+ 10 nM LH
FLAG-LHR WT
FLAG-LHR-APEX2
E
cAMP Production (% of LHR WT Emax)
Log [LH] M
EC50, nM ± SEM
Hill Slope ± SEM
Emax, %
LHR WT 0.50 ± 0.02 -1.6 ± 0.1 100
LHR-APEX2 0.30 ± 0.02 -2.1 ± 0.4 100
LHR-APEX2 no Tet
G
Rep 1
Rep 2
Plate:
H2O2:
LH (min):
Ponceau staining
F
n = 3
Biotin-phenol
LH
1 min
2 min
3 min
5 min
10 min
no LH
no LH
no H2O2
H2O2 (60s)
Quench
1. Lysis
2. Protein precipitation
3. On-bead pull-down
4. Digestion
5. TMT labeling
6. Sample pooling
Intensity
m/z
Interaction networks
Interaction profiles
8. Bioinformatics analysis
7. LC-MS/MS analysis and quantification

Figure 1. **Design of a proximity proteomics pipeline for LHR-APEX2**. **A**. Model summarizing current understanding of signaling and trafficking pathways of LHR activated by LH agonist. Upon activation, LHR couples to interactors that mediate its downstream effects including cAMP signaling, desensitization and internalization. Following internalization, LHR is trafficked to very early endosomes (VEE), smaller in size than early endosomes and lacking classical endosomal markers EEA1 and Rab5. From the VEE, LHR elicits downstream signaling cascades, including cAMP generation. LHR is then primarily rapidly recycled back intact to the plasma membrane, with a minor proportion sorted towards the EE and subsequently degradation [11]. However, the dynamic LHR interactome during endocytic trafficking to and from VEEs is currently unknown. **B**. To enable APEX2 proximity labeling, the APEX2 enzyme [28] is fused to the C-terminus of LHR where it can catalyze the formation of biotin-phenoxy radicals from biotin-phenol in the presence of hydrogen peroxide. These radicals persist only in close proximity (<20 nm) to LHR resulting in rapid biotinylation of nearby protein interactors, which can then be enriched, identified and quantified by quantitative mass spectrometry-based proteomics [34]. **C**. Timeline diagram of APEX2 proximity labeling along LHR endocytic signaling and trafficking route represented by its agonist-dependent functional 'clock' ranging from 1 up to 10 minutes post agonist addition. **D**. Validation of LHR-APEX2 expression and trafficking by confocal microscopy. FLAG-LHR WT HEK293 cells and Flp-In T-REx 293 FLAG-LHR-APEX2 cells were labeled with anti-FLAG antibody and non-treated (control) or treated with 10 nM LH for 10 min. Cells were fixed and stained with a secondary AlexaFluor 488 (AF488)-conjugated antibody. Shown is a representative frame from imaging of cells via confocal microscopy with a zoom-in inset (bottom right). Scale bar = 5 μm. Both untagged and APEX2-tagged LHR constructs exhibit comparable plasma membrane expression and LH-induced internalization into VEEs. **E**. Validation of LHR-APEX2 signaling by TR-FRET cAMP assay normalized to the LHR WT E_{max}. Dose-response cAMP curves for the FLAG-LHR WT HEK293 cells and tetracycline-induced Flp-In T-REx 293 LHR-APEX2 cells activated by various concentrations of LH produce comparable EC_{50} and E_{max} values. Non-induced cells do not respond to LH treatment. Data represent mean ± SEM (n = 3). **F**. APEX2 proximity labeling and mass spectrometry analysis workflow. Flp-In T-REx 293 LHR-APEX2 cells were pre-incubated with biotin-phenol, treated with LH for different time points, activated with hydrogen peroxide and quenched. Biotinylated proteins were pulled-down on streptavidin-coated beads, digested, labeled with the tandem isobaric mass tag (TMT) kit, analyzed and quantified by LC-MS/MS, followed by interactomics analysis. **G**. Biotinylated proteins analyzed by neutravidin-HRP western blot; increased biotinylation was observed for hydrogen peroxide-treated as opposed to untreated samples.

Quantitative proximity labeling enables dynamic activation-dependent LHR interactomics. To identify and quantify LH-responsive biotinylated proteins, we established a multi-step proteomics pipeline (**Figure 1F**). Enriched biotinylated proteins were digested on-bead, peptides quantified, concentrated and labeled with 7-plex isobaric tandem mass tags (TMT); peptides were combined per replicate, fractionated by alkaline reverse phase LC, separated by nanoscale reverse phase LC, and analyzed by tandem mass spectrometry (MS/MS). Samples with no hydrogen peroxide treatment were included as a background control and samples with no LH treatment were used as non-stimulated LHR-APEX2 controls. Across three independent experiments, 3584 proteins were

quantified in MaxQuant [38] (**Figure 2A**). As expected, >90% of proteins identified in no hydrogen peroxide-treated samples showed significantly lower protein abundances than hydrogen peroxide-treated samples, in agreement with western blotting data (**Figure S2A**). Proteins with comparable abundances across all samples including the "no hydrogen peroxide" background control were considered non-specific and omitted from further analysis in Perseus [39]. After log2 transformation, enriched protein abundances were normalized to LHR-APEX2 within each sample as an internal reference for labeling efficiency (**Figure S2B-E**). To focus analysis on the activation-dependent LHR-APEX2 interactome, proteins that either decreased or did not change in abundance following LH treatment were removed. Thus, all proteins were normalized per replicate to "no LH treatment" control, and subsequent analyses were carried out on proteins that displayed increased enrichment, and therefore potentially increased interaction with LHR, for at least one time point following receptor activation. In total, 2695 proteins were taken forward to KEGG pathway analysis using the DAVID online platform [40], confirming endocytosis as the most enriched pathway, as anticipated, with 128 proteins identified (**Figure 2B**). Similarly concordant enriched pathways included tight junctions, regulation of actin cytoskeleton, small G protein signal pathways (e.g. Rap1 and Ras) and the Hippo signaling pathway.

A time-resolved LHR interactome referenced to known LH-dependent LHR interactors. In order to establish reference points to identify and functionally classify novel LHR protein partners, we first analyzed the time-resolved interaction profiles of known ligand-dependent GPCR and/or LHR interactors. We found that profiles for multiple known agonist-dependent LHR interactors were consistent across three independent replicates, indicating remarkably robust reproducibility of proximity labeling. These included canonical GPCR interactors $G_{\alpha}s$ protein (GNAS), β-arrestin-2 (ARRB2), LHR C-terminal tail interactor GIPC1 [41], which followed profiles based on previously reported data using orthogonal methodologies [20,42,43], and known GPCR signaling and trafficking network components with interaction profiles similar to those found by other GPCR-APEX2 studies [29,30], including adenylate cyclases (ADCY), protein kinase A (PRKACA and PRKACB), clathrin-mediated endocytosis components (clathrin (CLTA, CLTB, CLTC), AP2, PICALM, EPN2) clustering in distinct phases (early, middle and late) following LH treatment (**Figure 2C-E**).

$G_{\alpha}s$ interaction was highest at the earliest time point (1 min) following LH treatment, but then fell below the basal level without LH stimulation at time points beyond 3 min, a finding supported by prior BRET-based studies showing that $G_{\alpha}s$ resides in close proximity, or "pre-coupled", to LHR [43,44] (**Figure 2C-E**). Additional $G_{\alpha}s$-cAMP signaling machinery enriched following agonist treatment included three adenylate cyclases ADCY3, ADCY6 and ADCY9 with the latter exhibiting a transient

interaction profile, and the catalytic subunits of protein kinase A (PRKACA and PRKACB) all showing up in the early interaction cluster (**Figure 2C-E**).

In contrast, LH-dependent association of LHR with β-arrestin-2 continued to increase following LH treatment and during $G_{\alpha}s$ uncoupling, and persisted through later time points consistent with previous resonance energy transfer studies demonstrating sustained LH-dependent interactions with β-arrestin-2 [42,43] (**Figure 2C-E**). Upon β-arrestin-2 recruitment, LHR is known to internalize via clathrin-coated pits (CCP), and indeed interaction with clathrin heavy and light chains (CLTA, CLTB, CLTC) peaked at 2 min following LH treatment, consistent with CCP formation coinciding with β-arrestin-2 recruitment (**Figure 2C-E**). Other enriched CCP components included AP2 complexes, PICALM, EPS15 and EPN1/2, consistent with previous studies using β2AR-APEX2 [29,30], with EPS15/EPN1 in the middle and EPN2/β-arrestin-2 in the late interaction clusters sharing a similar temporal profile (**Figure 2C,D**). ADP-ribosylation factor 6 (ARF6) exhibited a peak interaction profile following 1-2 min of LH stimulation, consistent with its role regulating early events in LHR internalization upstream of the scission of clathrin-coated pits [45] (**Figure 2C,D**). In contrast, interaction with ARF GTPase-activating protein GIT1 was sustained after peaking at 2 min, as previously described for β2AR [29] (**Figure 2C,D**).

As noted above, LHR is known to traffic through VEEs within 3 min to activate acute G protein signaling and enable subsequent rapid receptor recycling [19]. APPL1, the only adaptor protein previously shown to localize to VEEs, was not detected in these studies, likely due to limitations of abundance and sensitivity of mass spectrometry-based proteomics. However, the PDZ domain protein GIPC1 [41], which is necessary for LHR sorting into VEE [20], was enriched in agonist-treated samples, with a temporal profile strongly aligned with prior TIRF-microscopy imaging studies demonstrating GIPC1 recruitment during receptor clustering into CCPs, and dissociation following clathrin-coated vesicle disassembly and entry into VEEs [20] (**Figure 2C-E**).

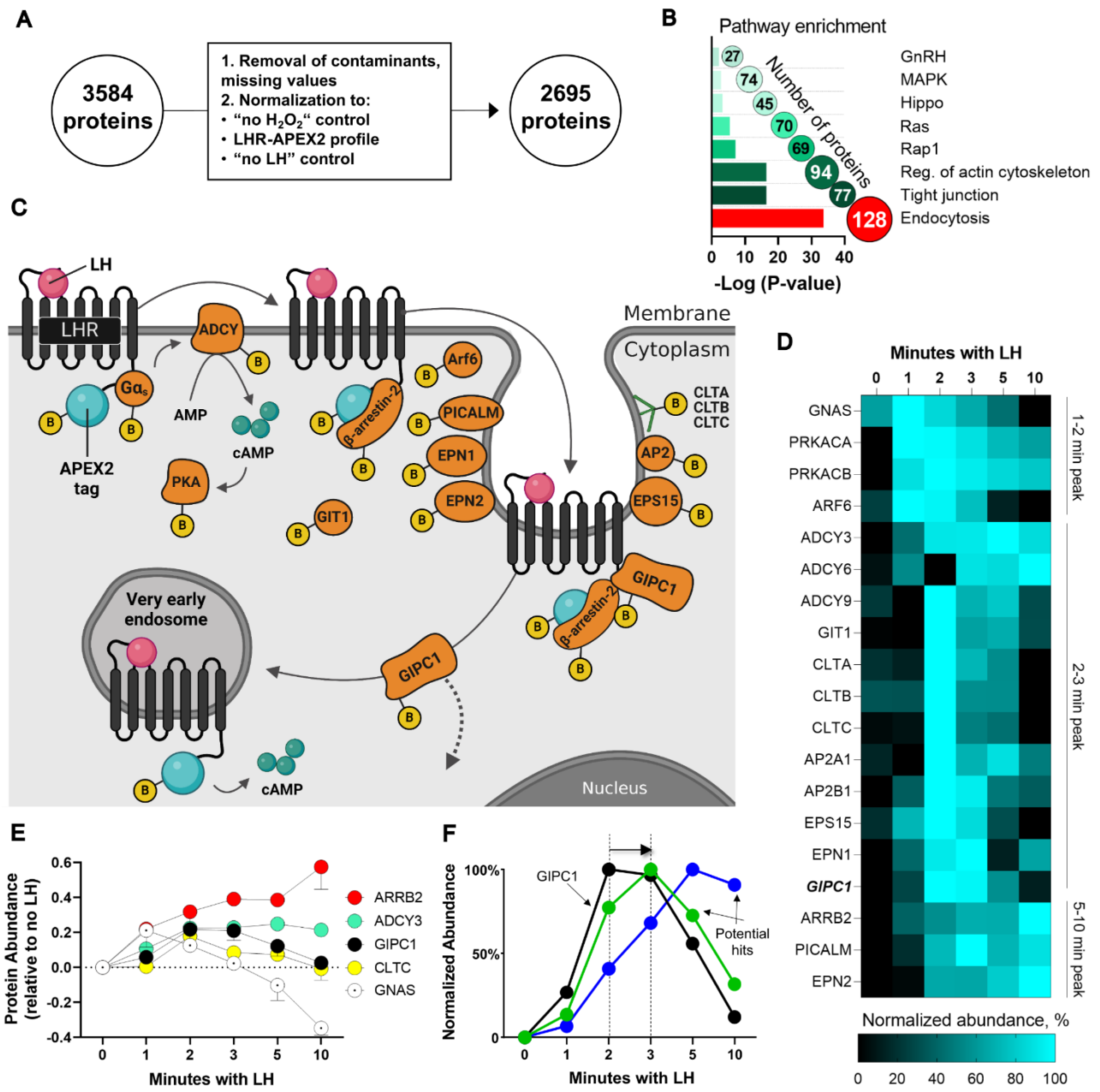

Figure 2. APEX2 captures known agonist-dependent LHR interactome. **A**. Protein filtration and normalization steps. For 3584 proteins found in MaxQuant [38], contaminants and missing values were removed in Perseus [39], and proteins enriched over background ("no H_2O_2" control) were normalized to the internal reference (LHR-APEX2 profile) and filtered based on the enrichment over the non-simulated ("no LH") control at any time point to focus on proteins which responded to LH treatment. **B**. Selected KEGG pathways enriched in proteomic datasets according to the DAVID online analysis platform [40]. Endocytosis is the most statistically enriched pathway in the dataset, with the highest number of proteins represented. **C**. Model summarizing known LHR interactors revealed by proteomic analysis. GIPC1 protein [20,41] must dissociate from the LHR C-terminal domain before LHR enters VEEs. **D**. Heatmap of interaction profiles for known LHR interactors. Enrichment level (abundance) for each protein across different time points was normalized to the non-stimulated ("no LH") control first, followed by normalization to its maximum and minimum enrichment signal. The profiles are ordered from early to late, according to the timepoint of their strongest interaction with LHR.

E. Temporal profiles of selected known LHR interactors. Enrichment level (abundance) for each protein across different time points was normalized to the non-stimulated ("no LH") control. Data represent mean ± SEM (n = 3). **F**. Schematic illustration of potential VEE-related hit interactor temporal profiles, set against the reference profile for GIPC1. Peak profiles for potential VEE-related hits are shifted to later timepoints compared to GIPC1, which peaks at 2 min and dissociates from the LHR C-terminus before LHR enters VEEs, providing a temporal reference point for VEE entry.

Leveraging the LHR-GIPC1 temporal profile to reveal novel LHR-APEX2 interactions. To demonstrate the potential for APEX2 proximity proteomics to identify new prospective regulatory interactors in a currently poorly understood pathway, we focused on previously unknown LHR-APEX2 interactors at the early endocytosis transition to VEEs. Given the requirement for GIPC1 to dissociate from LHR prior to VEE entry [20], the peak of LHR-GIPC1 interaction was used as a reference point for the start of VEE entry (**Figure 2F**). We applied a four-step bioinformatics data analysis workflow to identify potential new VEE-associated proteins with a peak enrichment right-shifted to later time points than GIPC1 (**Figure 2F** and **Figure 3b-e**). After initial filtering and normalization steps described before in **Figure 2A** (scheme repeated in **Figure 3a**), triplicate enrichment data for 2695 proteins was distributed into two groups arranged by the difference between their abundance values at the 2- and 3-min time points as shown on a difference plot (**Figure 3b**). Proteins in the first group peaked at the 1- or 2-min time points, and proteins in the second group peaked at or after the 3 min time point. Data for the 596 proteins in the second group were extracted (**Figure 3c**) and subjected to categorical enrichment analysis by GO term "Endo", performed in Perseus [39], resulting in 203 proteins bearing this term (**Figure 3d**). The most enriched categories after analysis were "clathrin-coated vesicle", "coated membrane", and "vesicle coat". To define a focused subset of hits for functional studies, these 203 proteins were subjected to manual selection based on their likely functional relationship to VEEs. These included proteins with association to core endosomal functions such as endosome fusion, acidification and membrane protein sorting (e.g. Rabs, sorting nexins, V-type ATPases), cAMP generation and cAMP/PKA effectors or role in signalosomes (e.g. adenylate cyclases, AKAPs, Ras-related GTPases), and association with cytoskeletal machinery and peripheral vesicles (e.g. ARF6 GTPase activating proteins). This led to 49 selected hits arranged by their interaction clusters (**Figure 3e**), which were taken forward for further study.

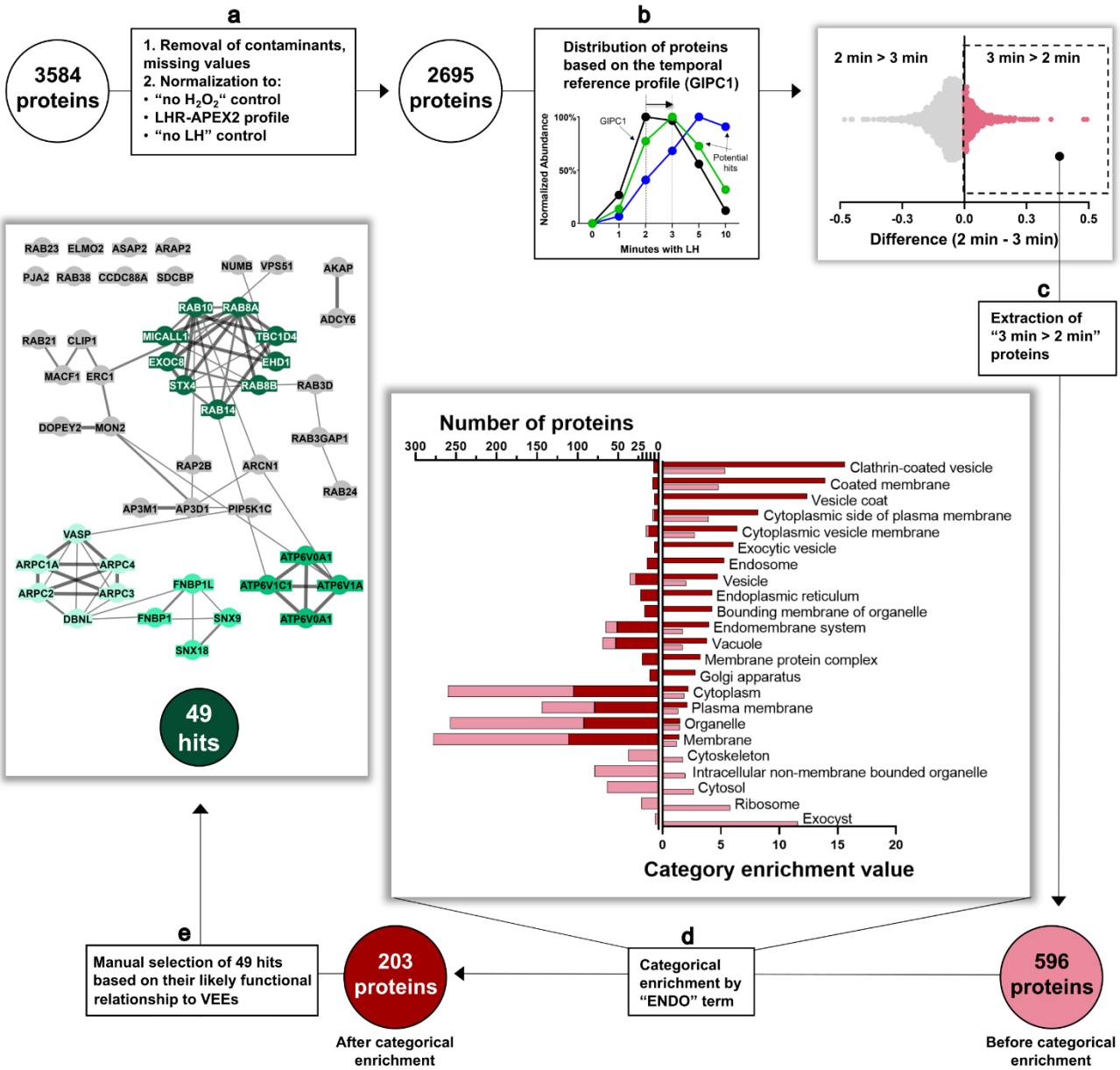

Figure 3. **Interactomics data analysis workflow based on the GIPC1 temporal reference profile**. **a.** For 3584 proteins found in MaxQuant [38], contaminants and missing values were removed in Perseus [39], and proteins enriched over background ("no H_2O_2" control) were normalized to the internal reference (LHR-APEX2 profile) and filtered based on enrichment over the non-simulated ("no LH") control at any time point to focus on proteins which responded to LH treatment. **b**. Using the GIPC1 temporal profile as a reference, data for 2695 proteins were distributed in two groups arranged by the difference between their abundance values at the 2 and 3 min time points, as shown on the difference plot. **c-d.** Data for the 596 proteins in the second group were extracted and subjected to categorical enrichment analysis by GO term "Endo", performed in Perseus, resulting in 203 proteins bearing this term. The graph shows category enrichment value for proteins before (596, pink) and after (203, burgundy) enrichment step on the right with corresponding protein numbers on the left. **e**. The enriched 203 proteins were subjected to manual selection based on their likely functional relationship to VEEs, leading to 49 selected hits. The last panel shows 49 selected hits arranged by their

interaction clusters derived from STRING web-based platform [46] (figure adapted from Cytoscape (3.10.0) [47]). The edges represent STRING database score. A more detailed review of the data analysis workflow is provided in Supplementary Materials.

Identification of functional interactors of LHR modulating $G_{\alpha}s$ signal transduction. To functionally annotate potential modulators of LHR signaling we screened all 49 selected hits and 5 controls (non-targeting control (NTC), β-arrestin-2 (ARRB2), the VEE proteins APPL1 and GIPC1 and $G_{\alpha}s$ (the essential mediator of $G_{\alpha}s$-coupled signaling, GNAS)) by RNA interference (RNAi) knock-down for changes in cAMP produced by WT LHR, under LH stimulation. FLAG-LHR WT HEK293 stable cells were reverse transfected with an siRNA library and grown for 96 hours. Screens were performed at two different LH concentrations to maximize the detection window for knock-downs that increase cAMP levels (3 nM LH, Screen 1, **Figure 4A**) or reduce cAMP levels (10 nM LH, Screen 2, **Figure 4B**). To focus our analysis on knock-downs which did not cause major disruption in cellular function, each well was additionally analyzed manually by phase contrast microscopy, and instances with altered cell viability or morphology were not considered further (shown as discarded points on **Figure 4A-B**). GNAS knock-down was used as a positive control for signal inhibition and exhibited nearly 100% reduction in LH-mediated cAMP generation, as expected for the $G_{\alpha}s$-coupled LHR. The highest-ranking hits found in both screens which reduced cAMP generation on knock-down, and therefore are potential *positive* modulators of LHR signaling, were RAP2B, EHD1, ARPC1A, MON2 with additional ARPC3, ELMO2, DBNL, SNX18, AP3M1 found in either Screen 1 or 2; the highest-ranking hits that increased cAMP generation on knock-down in both screens were RAB38, RAB23, ATP6V0A1, SNX9 with additional TBC1D4, AKAP5, AP3D1, RAB24, MACF1 found in either Screen 1 or 2, and were considered potential *negative* modulators of signaling.

We next further validated the impact on LHR-mediated cAMP production for knock-down of the two strongest validated cAMP-modulating hits, RAP2B and RAB38, following stimulation with 1 nM, 3 nM or 10 nM LH (**Figure 4C**). The LH-dependent cAMP levels produced by RAP2B knock-down cells was ~2.5 times less than in control cells, whereas for RAB38 knock-down the increase was ~2.4 times compared to the control cells, suggesting a significant effect on agonist-mediated LHR signaling function. The impact on the kinetics of cAMP signaling was assessed by employing the cAMP GloSensor™ reporter [48] which demonstrated that the increase (via RAB38 knock-down) or decrease (via RAP2B knock-down) in agonist-dependent LHR cAMP signaling was sustained over an extended period post-stimulation with LH (**Figure 4D,E**). Comparison of heatmaps of interaction profiles for knock-downs leading to cAMP decrease or increase indicated that LHR-APEX2 interactors with a potential positive effect on LHR signaling (i.e. which lead to decreased cAMP signaling on knock-down) exhibit a profile with a peak of association at 3 min followed by

dissociation, whereas the majority of interactors with a potential negative regulatory effect (i.e. which lead to increased cAMP signaling on knock-down) exhibit sustained proximity to LHR up to and beyond 5 min post-stimulation with LH (**Figures 4F,G**).

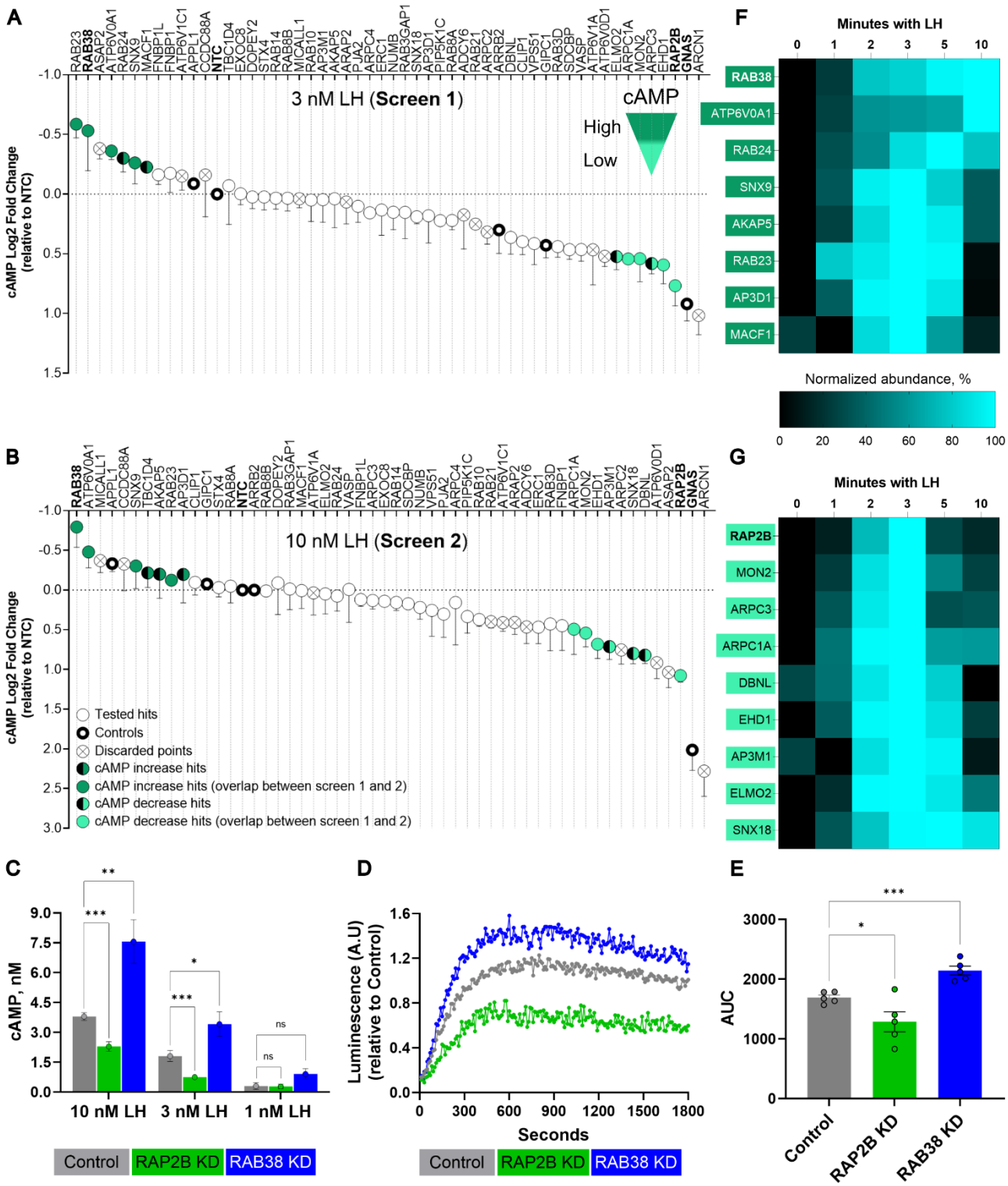

Figure 4. Functional analysis of 49 potential LHR interactors by knock-down and cAMP assays. FLAG-LHR HEK293 stable cells were transfected with an siRNA library for 96 h and stimulated with LH for 5 min (3 nM LH for Screen 1 (**A**) and 10 nM LH for Screen 2 (**B**)). Intracellular cAMP levels were measured from cell

lysates by a TR-FRET cAMP assay. Controls included a non-targeting control (NTC) siRNA, and siRNA for GNAS (the essential mediator of G_{α}s-coupled signaling), the VEE proteins APPL1 and GIPC1, and β-arrestin-2 (ARRB2). Responses were normalized to the NTC value per each replicate, transformed to Log2 and the plot is ranked from high cAMP (dark-green/black circles) to low cAMP (light-green/black circles). Hits found in both Screens 1 and 2 are shown as dark-green and light-green circles. Hits which exhibited negative effects on cell morphology and/or viability after knock-down are shown as discarded points (cross). The most changed hits present in both screens were RAP2B and RAB38. Data represent mean ± SEM (n = 3). **C**. cAMP generated by RAP2B and RAB38 knock-downs (KD) compared to NTC (Control) upon stimulation with 1 nM, 3 nM or 10 nM LH for 5 min. cAMP concentration was interpolated from TR-FRET signal using a cAMP standard curve. Data represent mean ± SEM (n = 3). Statistical analysis was performed by unpaired Student's t-test: ns > 0.05, *p < 0.05, **p < 0.01, ***p < 0.001. **D-E**. Live cAMP production indicated by GloSensor [48] luminescence over 30 minutes by RAP2B and RAB38 knock-downs (KD) following stimulation with 10 nM LH. Representative kinetic trace, values normalized to NTC (Control) measurement at 30 minutes (**D**). Data represent mean of the area under the curve (AUC) ± SEM (n = 5). Statistical analysis was performed by unpaired Student's t-test: *p < 0.05, ***p < 0.001. (**E**). **F**. Heatmap of interaction profiles for knock-downs leading to increased cAMP (hits are putative *negative* regulators of LHR signaling); protein enrichment across timepoints was first normalized to unstimulated ("no LH") control, followed by normalization to the maximum and minimum enrichment signal for each protein. The profiles show a trend of a sustained interaction with LHR, with interactors staying in proximity after 3 and 5 min. **G**. Heatmap of interaction profiles for knock-downs leading to decreased cAMP (hits are putative *positive* regulators of LHR signaling). Profiles show a trend of a sharp interaction with LHR between 2-3 min upon LH stimulation.

RAP2B knock-down reroutes LHR to early endosomes. RAP2B is a member of the Ras-related superfamily of small GTPases, with a known role as a *downstream* effector of cAMP/EPAC signalosomes [49]. Activation of RAP2B by EPAC leads to phospholipase C-epsilon signaling, but RAP2B has not previously been reported to function upstream of the cAMP pathway in generating, promoting or maintaining cAMP signaling. We have previously demonstrated that acute LHR-cAMP signaling requires receptor internalization [19], and to further clarify a potential novel role of RAP2B we explored the impact of RAP2B knock-down on LHR internalization and trafficking by confocal microscopy. FLAG-LHR HEK293 stable cells were transfected with non-targeting control (NTC), GIPC1 or RAP2B siRNA and plated onto PDL-coated coverslips 72 h post-transfection. After a further 24 h, cells were treated with 10 nM LH for 5 min, stripped, fixed, and labeled with secondary anti-FLAG and anti-EEA1 antibodies, followed by confocal microscopy imaging. It is known that following 10 min LH treatment, LHR rapidly internalizes primarily to a VEE compartment, and that disruption of this sorting via loss of GIPC1 redirects receptors to the early endosome and to a degradative pathway [20,41]. Therefore, colocalization of LHR with the early endosomal marker EEA1 was measured following knock-down of RAP2B or GIPC1 to assess the impact on LHR endosomal trafficking. Interestingly, knock-down of either RAP2B or GIPC1 increased colocalization of LHR with

EEA1 by approximately 2-fold compared to NTC (Control) (**Figure 5A,B**). These data suggest that in the absence of RAP2B LHR is rerouted to early endosomes, implying that RAP2B may play a role in promoting LHR trafficking to the VEE (**Figure 5C**).

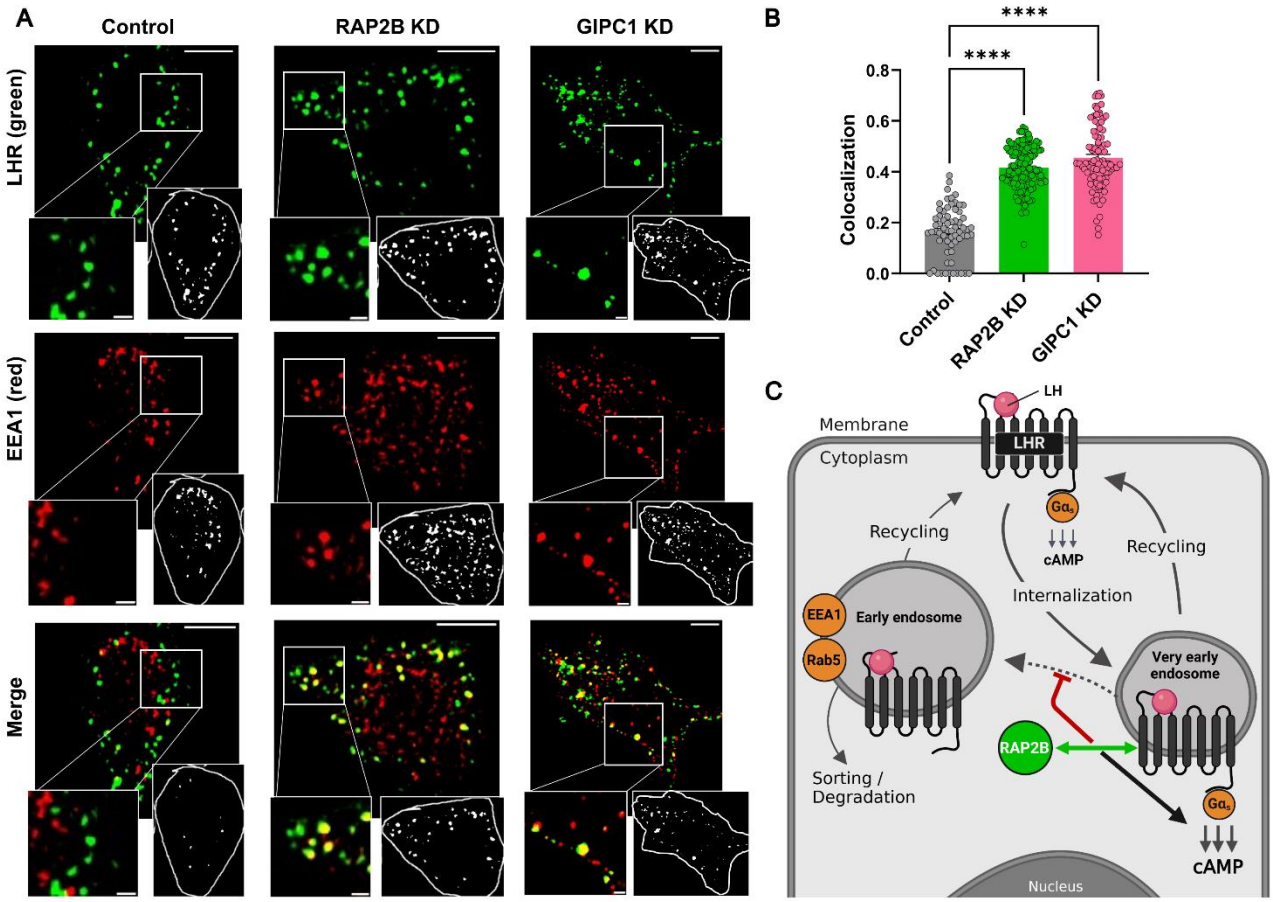

Figure 5. **RAP2B knock-down reroutes LHR to early endosomes**. **A**. Confocal images of FLAG-LHR HEK293 stable cells under three knock-down (KD) conditions: non-targeting control, RAP2B and GIPC1. FLAG-LHR was labeled with anti-FLAG antibody and treated with 10 nM LH for 10 min. Cells were stripped, fixed, permeabilized and stained with an anti-EEA1 antibody, followed by secondary AF594- and AF488-conjugated antibodies. Shown is a representative frame from imaging of cells via confocal microscopy with a zoom-in inset (bottom left). A representative single cell output image with threshold mask for each channel and colocalized pixels is shown in another inset (bottom right). Scale bar = 5 µm. Scale bar in the zoom-in inset = 1 µm. **B**. Quantification of colocalization between LHR channel (green) and EEA1 channel (red) that translates to how many LHR-containing endosomes are also EEA1-positive. The Manders colocalization coefficient is shown under three knock-down conditions. Z-slices were considered separately; n = 10 cells per condition; 15 z-slices per each cell. Data represent mean ± SEM. Statistical analysis was performed by unpaired Student's t-test: ****$p < 0.0001$. **C**. A mechanistic hypothesis for the role of RAP2B interaction with LHR in very early endosomes (VEE). Our data suggest that RAP2B may have direct roles in stimulating LHR cAMP signaling from VEE as well as inhibiting fusion of LHR-containing VEE with early endosomes.

Discussion

Quantitative proximity proteomics [26,27] has recently emerged as a cutting edge technology to capture the complexity of GPCR networks at a spatial and temporal level [29-31,36,50]. However, interrogation of these activation-dependent interactomes resolved on a scale of minutes can be challenging, raising significant demands on robust data analysis [27], and to date this approach has been mostly applied to well-understood GPCRs with a largely established interactome. In this study, we applied quantitative APEX2 [28] proximity proteomics to define the LHR interaction network on a minute-to-minute timescale. We developed an integrated experimental and analytical methodology which combines highly reproducible quantitative TMT-based proteomics with temporal reference profiles for key interactors to identify novel LHR interactors in a specific spatial compartment, the VEE [19,20]. Although applied here to LHR, we expect that the pipeline developed will be applicable to any GPCR which undergoes rapid early and post-endocytic events, and/or where a receptor traverses multiple subcellular compartments.

Using LH stimulation time points based on established LHR signaling kinetics, endocytosis and trafficking into and from VEEs [19,20], proximity proteomics identified almost ~2700 LH-dependent interactions, which is a similar range to previously reported studies applying APEX2 [29,35]. Only a subset of these proteins are likely to be direct interactors of LHR with the potential to functionally regulate LHR activity, since APEX2 labeling also captures indirect interactors within a 20 nm radius. A robust analytical pipeline was essential to overcome several confounding features of proximity labeling. First, the relative abundance of a particular protein in the interactome does not necessarily strongly correlate with physical interaction; for example, GIPC1 and clathrin heavy chain were similarly enriched (**Figure S2F**) despite the former having a known direct interaction with LHR [20,41]. Second, bona fide interactors may not be identified due to the intrinsic limitations of mass spectrometry to detect low abundance proteins or which lack proteotypic tryptic peptides. For example, APPL1 was not identified in this study. Third, the shortest temporal resolution of APEX2 is currently limited to ca. 1 min, and therefore may not fully capture events at even shorter timescales. Fourth, as a membrane protein, LHR-APEX2 would be expected to be present in various subcellular compartments (e.g. ER, Golgi) in addition to the plasma membrane and endosomes, potentially contributing to the challenges of interactome deconvolution [51]. Finally, affinity purification also generates background due to nonspecific protein interactions with the resin. Therefore, TMT-labeled controls ("no H_2O_2" and "no LH") and a cascade of filtering and normalization steps were required to provide a cut-off and select high confidence LHR-interacting proteins for further analysis (**Figure 2A**). All protein profiles were normalized to the LHR-APEX2 abundance profile as an internal standard per replicate, to account for any variations during sample processing, which proved to be the critical step in our analysis as demonstrated by the representative protein profiles before and after normalization (**Figure S2B-E**). Our refined pipeline approach robustly captured both direct and

indirect known LHR interactors with excellent spatiotemporal resolution, including several with transient or low-affinity interactions, such as G protein signal transducers (**Figure 2** and **Figure S3**), β-arrestin-2 and ARF6 (**Figure 2**). The HEK293 cell model also enabled identification of interactors specifically relevant to physiological LHR signaling, including Hippo signaling components involved in ovarian granulosa cell to luteal cell differentiation [52] (**Figure S4**). We focused on functional validation of VEE compartment interactions in the present work due to the VEE importance for LHR signaling and trafficking. However, the dynamic interactomic datasets generated here may also prove a valuable resource for future mapping of the landscape of LH-induced LHR interactions at the plasma membrane, during formation of CCPs, and other rapid activation-dependent events which are currently poorly characterized for this receptor.

The application of a temporal profile for a known interactor (GIPC1 in the present study) as an internal reference for functional annotation of dynamic networks when GPCR pharmacological tools (i.e. agonists and antagonists) are limited, offers a powerful alternative to other approaches which employed comparative proteomics (e.g., agonist vs antagonist; agonist vs biased agonist [29,36]) or spatial references requiring complex analysis across distantly related APEX2 datasets [30]. Previous biochemical and cell biology studies have demonstrated that GIPC1 interaction with the LHR C-terminal tail occurs during LHR clathrin-mediated endocytosis, dissociating prior to entering the VEE compartment [20] (**Figure 2C**). The exquisite temporal resolution of APEX2 labeling enabled us to exclude LHR interactors with maximum abundances at timepoints prior to GIPC1 dissociation and focus on plausible regulators of VEE trafficking and/or signaling (**Figure 3**). Interestingly, our functional studies identified two contrasting interaction profiles, with putative positive regulators of LHR signaling showing interaction profiles peaking at 3 min post-activation (**Figure 4G**), whereas the majority of putative negative regulators maintained their proximity from 3 min across the 10 min ligand stimulation window of the experiment (**Figure 4F**). This temporal profile of negative regulators may suggest such LHR complexes function to switch off signal activity prior to receptor recycling back to the plasma membrane, given LHR recycling has been captured within this same time frame [19].

Two novel LHR interactors, RAP2B and RAB38 were found as putative positive and negative regulators of LHR signaling, respectively, with RAP2B also regulating endosomal distribution of LHR. RAB38 is a member of the family of Rab small GTPases, well known for their roles in regulating membrane trafficking, and has been previously studied in the context of melanosome biogenesis [53,54]. Prior studies of the classic early endosomal RAB5 demonstrated no role in VEE generation or impact on LHR trafficking [20], and the identification of a distinct Rab family member in this study which may promote LHR-mediated cAMP signaling from the VEE is a significant step towards a mechanistic understanding of VEE-dependent signaling, and an important topic for future studies. RAP2B is a member of the Ras-related family of small G proteins. While this protein has been

reported to be a downstream regulator of cAMP signaling from certain G_{α}s-coupled GPCRs, where the cAMP effector EPAC with RAP2B activates calcium signaling via PLC-epsilon [55], this is the first report of a potential role for RAP2B upstream of cAMP generation. In addition, RAP2B exhibits parallels with the known activity of GIPC1 in retaining LHR within the VEE. However, in contrast to GIPC1, RAP2B also seems to be a positive regulator of LHR-cAMP signaling, a novel function which may be independent from its ability to regulate endosomal sorting of LHR.

Overall, we present an APEX2 pipeline optimized for the study of GPCRs, and likely also other membrane receptors, with minimal existing pharmacological tools, spatial markers and/or known protein interactors. Our findings highlight the intricate complexity of GPCR interactomes and illustrate the importance of developing methods to deconvolute this complexity. We expect that these and similar approaches will enable broader applicability of proximity labeling to accelerate fundamental discovery research for the large superfamily of GPCRs.

Acknowledgements

We acknowledge funding support from the Laboratory for Synthetic Chemistry and Chemical Biology under the Health@InnoHK Program of The Government of Hong Kong Special Administrative Region of the People's Republic of China and the Biotechnology and Biological Sciences Research Council (BBSRC), grants BB/S001565/1 and BB/V006142/1. Schematics were created in BioRender.com. We would like to thank Prof. Mark von Zastrow (Univ. California, San Francisco, USA), Prof Gunther Schmalzing (RWTH Aachen Univ., Germany), Prof Ali Tavassoli (Univ. Southampton, UK) and Dr Kim Jonas (King’s College London, UK) for providing certain plasmids. We would like to thank Shabbir Ahmed (Leica Microsystems) and Tracey Williams (Leica Microsystems) for access and assistance with Mica (Zeiss) imaging. We would like to thank Tate group members for assistance and insightful discussions and Erika Bernardini for help with cell culture. We would like to acknowledge Dr Roman Fedoryshchak for his assistance with confocal microscopy and critical reading of this manuscript.

Author contributions

MMS, EWT and ACH conceptualized the study, obtained funding and provided resources for the study. ARW carried out GloSensor assay and analysis. MMS developed and carried out all other experiments in this study, developed bioinformatics analysis pipeline, performed functional studies, confocal microscopy, data analysis and made all the figures. RR contributed to confocal microscopy studies. DC supervised proteomics set up and provided guidance. JH contributed to some of the proteomics analysis steps and generated the Cytoscape figure panel. MMS, ACH and EWT wrote

the original draft of the manuscript, and all authors provided comments, reviewed, and edited the final manuscript.

Conflicts of interest

The authors declare the following financial interests/personal relationships which may be considered as potential competing interests. EWT is a founder, shareholder, and director of Myricx Pharma Ltd. The remaining authors declare that they have no known competing financial interests or personal relationships that could have appeared to influence the work reported in this article.

References

1. Rosenbaum, D.M., Rasmussen, S.G., and Kobilka, B.K. (2009). The structure and function of G-protein-coupled receptors. Nature *459*, 356-363. 10.1038/nature08144.
2. Ritter, S.L., and Hall, R.A. (2009). Fine-tuning of GPCR activity by receptor-interacting proteins. Nat Rev Mol Cell Biol *10*, 819-830. 10.1038/nrm2803.
3. Lefkowitz, R.J. (2013). A brief history of G-protein coupled receptors (Nobel Lecture). Angew Chem Int Ed Engl *52*, 6366-6378. 10.1002/anie.201301924.
4. Shchepinova, M.M., Hanyaloglu, A.C., Frost, G.S., and Tate, E.W. (2020). Chemical biology of noncanonical G protein-coupled receptor signaling: Toward advanced therapeutics. Curr Opin Chem Biol *56*, 98-110. 10.1016/j.cbpa.2020.04.012.
5. Nurnberg, B., Beer-Hammer, S., Reisinger, E., and Leiss, V. (2024). Non-canonical G protein signaling. Pharmacol Ther *255*, 108589. 10.1016/j.pharmthera.2024.108589.
6. Farooq, Z., Howell, L.A., and McCormick, P.J. (2022). Probing GPCR Dimerization Using Peptides. Front Endocrinol (Lausanne) *13*, 843770. 10.3389/fendo.2022.843770.
7. Farran, B. (2017). An update on the physiological and therapeutic relevance of GPCR oligomers. Pharmacol Res *117*, 303-327. 10.1016/j.phrs.2017.01.008.
8. Thomsen, A.R.B., Jensen, D.D., Hicks, G.A., and Bunnett, N.W. (2018). Therapeutic Targeting of Endosomal G-Protein-Coupled Receptors. Trends Pharmacol Sci *39*, 879-891. 10.1016/j.tips.2018.08.003.
9. Ribeiro-Oliveira, R., Vojtek, M., Goncalves-Monteiro, S., Vieira-Rocha, M.S., Sousa, J.B., Goncalves, J., and Diniz, C. (2019). Nuclear G-protein-coupled receptors as putative novel pharmacological targets. Drug Discov Today *24*, 2192-2201. 10.1016/j.drudis.2019.09.003.
10. Jong, Y.I., Harmon, S.K., and O'Malley, K.L. (2018). GPCR signalling from within the cell. Br J Pharmacol *175*, 4026-4035. 10.1111/bph.14023.
11. Sposini, S., and Hanyaloglu, A.C. (2018). Driving gonadotrophin hormone receptor signalling: the role of membrane trafficking. Reproduction *156*, R195-R208. 10.1530/REP-18-0423.
12. De Pascali, F., and Reiter, E. (2018). beta-arrestins and biased signaling in gonadotropin receptors. Minerva Ginecol *70*, 525-538. 10.23736/S0026-4784.18.04272-7.
13. Ascoli, M., Fanelli, F., and Segaloff, D.L. (2002). The lutropin/choriogonadotropin receptor, a 2002 perspective. Endocr Rev *23*, 141-174. 10.1210/edrv.23.2.0462.
14. Breen, S.M., Andric, N., Ping, T., Xie, F., Offermans, S., Gossen, J.A., and Ascoli, M. (2013). Ovulation involves the luteinizing hormone-dependent activation of G(q/11) in granulosa cells. Mol Endocrinol *27*, 1483-1491. 10.1210/me.2013-1130.
15. Donadeu, F.X., and Ascoli, M. (2005). The differential effects of the gonadotropin receptors on aromatase expression in primary cultures of immature rat granulosa cells are highly dependent on the density of receptors expressed and the activation of the inositol phosphate cascade. Endocrinology *146*, 3907-3916. 10.1210/en.2005-0403.
16. Jeppesen, J.V., Kristensen, S.G., Nielsen, M.E., Humaidan, P., Dal Canto, M., Fadini, R., Schmidt, K.T., Ernst, E., and Yding Andersen, C. (2012). LH-receptor gene expression in human granulosa and cumulus cells from antral and preovulatory follicles. J Clin Endocrinol Metab *97*, E1524-1531. 10.1210/jc.2012-1427.
17. Galet, C., and Ascoli, M. (2008). Arrestin-3 is essential for the activation of Fyn by the luteinizing hormone receptor (LHR) in MA-10 cells. Cell Signal *20*, 1822-1829. 10.1016/j.cellsig.2008.06.005.
18. Mukherjee, S., Gurevich, V.V., Jones, J.C., Casanova, J.E., Frank, S.R., Maizels, E.T., Bader, M.F., Kahn, R.A., Palczewski, K., Aktories, K., and Hunzicker-Dunn, M. (2000). The ADP ribosylation factor nucleotide exchange factor ARNO promotes beta-arrestin release necessary for luteinizing hormone/choriogonadotropin receptor desensitization. Proc Natl Acad Sci U S A *97*, 5901-5906. 10.1073/pnas.100127097.
19. Sposini, S., Jean-Alphonse, F.G., Ayoub, M.A., Oqua, A., West, C., Lavery, S., Brosens, J.J., Reiter, E., and Hanyaloglu, A.C. (2017). Integration of GPCR Signaling and Sorting from Very Early Endosomes via Opposing APPL1 Mechanisms. Cell Rep *21*, 2855-2867. 10.1016/j.celrep.2017.11.023.

20. Jean-Alphonse, F., Bowersox, S., Chen, S., Beard, G., Puthenveedu, M.A., and Hanyaloglu, A.C. (2014). Spatially restricted G protein-coupled receptor activity via divergent endocytic compartments. J Biol Chem *289*, 3960-3977. 10.1074/jbc.M113.526350.
21. Caengprasath, N., and Hanyaloglu, A.C. (2019). Hardwiring wire-less networks: spatially encoded GPCR signaling in endocrine systems. Current Opinion in Cell Biology *57*, 77-82. https://doi.org/10.1016/j.ceb.2018.12.009.
22. von Zastrow, M. (2021). Proteomic Approaches to Investigate Regulated Trafficking and Signaling of G Protein-Coupled Receptors. Mol Pharmacol *99*, 392-398. 10.1124/molpharm.120.000178.
23. Seath, C.P., Trowbridge, A.D., Muir, T.W., and MacMillan, D.W.C. (2021). Reactive intermediates for interactome mapping. Chem Soc Rev *50*, 2911-2926. 10.1039/d0cs01366h.
24. Gingras, A.C., Abe, K.T., and Raught, B. (2019). Getting to know the neighborhood: using proximity-dependent biotinylation to characterize protein complexes and map organelles. Curr Opin Chem Biol *48*, 44-54. 10.1016/j.cbpa.2018.10.017.
25. Qin, W., Cho, K.F., Cavanagh, P.E., and Ting, A.Y. (2021). Deciphering molecular interactions by proximity labeling. Nat Methods *18*, 133-143. 10.1038/s41592-020-01010-5.
26. Kim, D.I., and Roux, K.J. (2016). Filling the Void: Proximity-Based Labeling of Proteins in Living Cells. Trends Cell Biol *26*, 804-817. 10.1016/j.tcb.2016.09.004.
27. Lundberg, E., and Borner, G.H.H. (2019). Spatial proteomics: a powerful discovery tool for cell biology. Nat Rev Mol Cell Biol *20*, 285-302. 10.1038/s41580-018-0094-y.
28. Lam, S.S., Martell, J.D., Kamer, K.J., Deerinck, T.J., Ellisman, M.H., Mootha, V.K., and Ting, A.Y. (2015). Directed evolution of APEX2 for electron microscopy and proximity labeling. Nat Methods *12*, 51-54. 10.1038/nmeth.3179.
29. Paek, J., Kalocsay, M., Staus, D.P., Wingler, L., Pascolutti, R., Paulo, J.A., Gygi, S.P., and Kruse, A.C. (2017). Multidimensional Tracking of GPCR Signaling via Peroxidase-Catalyzed Proximity Labeling. Cell *169*, 338-349.e311. https://doi.org/10.1016/j.cell.2017.03.028.
30. Lobingier, B.T., Hüttenhain, R., Eichel, K., Miller, K.B., Ting, A.Y., von Zastrow, M., and Krogan, N.J. (2017). An Approach to Spatiotemporally Resolve Protein Interaction Networks in Living Cells. Cell *169*, 350-360.e312. https://doi.org/10.1016/j.cell.2017.03.022.
31. Civciristov, S., Huang, C., Liu, B., Marquez, E.A., Gondin, A.B., Schittenhelm, R.B., Ellisdon, A.M., Canals, M., and Halls, M.L. (2019). Ligand-dependent spatiotemporal signaling profiles of the μ-opioid receptor are controlled by distinct protein-interaction networks. Journal of Biological Chemistry *294*, 16198-16213. 10.1074/jbc.RA119.008685.
32. Lobingier, B.T., and von Zastrow, M. (2019). When trafficking and signaling mix: How subcellular location shapes G protein-coupled receptor activation of heterotrimeric G proteins. Traffic *20*, 130-136. 10.1111/tra.12634.
33. Ward, R.J., Alvarez-Curto, E., and Milligan, G. (2011). Using the Flp-In T-Rex system to regulate GPCR expression. Methods Mol Biol *746*, 21-37. 10.1007/978-1-61779-126-0_2.
34. Hung, V., Udeshi, N.D., Lam, S.S., Loh, K.H., Cox, K.J., Pedram, K., Carr, S.A., and Ting, A.Y. (2016). Spatially resolved proteomic mapping in living cells with the engineered peroxidase APEX2. Nat Protoc *11*, 456-475. 10.1038/nprot.2016.018.
35. Perez Verdaguer, M., Zhang, T., Surve, S., Paulo, J.A., Wallace, C., Watkins, S.C., Gygi, S.P., and Sorkin, A. (2022). Time-resolved proximity labeling of protein networks associated with ligand-activated EGFR. Cell Rep *39*, 110950. 10.1016/j.celrep.2022.110950.
36. Pfeiffer, C.T., Wang, J., Paulo, J.A., Jiang, X., Gygi, S.P., and Rockman, H.A. (2021). Mapping Angiotensin II Type 1 Receptor-Biased Signaling Using Proximity Labeling and Proteomics Identifies Diverse Actions of Biased Agonists. J Proteome Res *20*, 3256-3267. 10.1021/acs.jproteome.1c00080.
37. Chapman-Smith, A., and Cronan, J.E. (1999). Molecular biology of biotin attachment to proteins. J Nutr *129*, 477S-484S. 10.1093/jn/129.2.477S.
38. Cox, J., and Mann, M. (2008). MaxQuant enables high peptide identification rates, individualized p.p.b.-range mass accuracies and proteome-wide protein quantification. Nat Biotechnol *26*, 1367-1372. 10.1038/nbt.1511.

39. Tyanova, S., Temu, T., Sinitcyn, P., Carlson, A., Hein, M.Y., Geiger, T., Mann, M., and Cox, J. (2016). The Perseus computational platform for comprehensive analysis of (prote)omics data. Nat Methods *13*, 731-740. 10.1038/nmeth.3901.
40. Dennis, G., Jr., Sherman, B.T., Hosack, D.A., Yang, J., Gao, W., Lane, H.C., and Lempicki, R.A. (2003). DAVID: Database for Annotation, Visualization, and Integrated Discovery. Genome Biol *4*, P3.
41. Hirakawa, T., Galet, C., Kishi, M., and Ascoli, M. (2003). GIPC binds to the human lutropin receptor (hLHR) through an unusual PDZ domain binding motif, and it regulates the sorting of the internalized human choriogonadotropin and the density of cell surface hLHR. J Biol Chem *278*, 49348-49357. 10.1074/jbc.M306557200.
42. Riccetti, L., Yvinec, R., Klett, D., Gallay, N., Combarnous, Y., Reiter, E., Simoni, M., Casarini, L., and Ayoub, M.A. (2017). Human Luteinizing Hormone and Chorionic Gonadotropin Display Biased Agonism at the LH and LH/CG Receptors. Sci Rep *7*, 940. 10.1038/s41598-017-01078-8.
43. Ayoub, M.A., Landomiel, F., Gallay, N., Jegot, G., Poupon, A., Crepieux, P., and Reiter, E. (2015). Assessing Gonadotropin Receptor Function by Resonance Energy Transfer-Based Assays. Front Endocrinol (Lausanne) *6*, 130. 10.3389/fendo.2015.00130.
44. Jonas, K.C., Fanelli, F., Huhtaniemi, I.T., and Hanyaloglu, A.C. (2015). Single molecule analysis of functionally asymmetric G protein-coupled receptor (GPCR) oligomers reveals diverse spatial and structural assemblies. J Biol Chem *290*, 3875-3892. 10.1074/jbc.M114.622498.
45. Kanamarlapudi, V., Thompson, A., Kelly, E., and López Bernal, A. (2012). ARF6 activated by the LHCG receptor through the cytohesin family of guanine nucleotide exchange factors mediates the receptor internalization and signaling. J Biol Chem *287*, 20443-20455. 10.1074/jbc.M112.362087.
46. Szklarczyk, D., Gable, A.L., Nastou, K.C., Lyon, D., Kirsch, R., Pyysalo, S., Doncheva, N.T., Legeay, M., Fang, T., Bork, P., et al. (2021). The STRING database in 2021: customizable protein-protein networks, and functional characterization of user-uploaded gene/measurement sets. Nucleic Acids Res *49*, D605-D612. 10.1093/nar/gkaa1074.
47. Su, G., Morris, J.H., Demchak, B., and Bader, G.D. (2014). Biological network exploration with Cytoscape 3. Curr Protoc Bioinformatics *47*, 8 13 11-24. 10.1002/0471250953.bi0813s47.
48. Binkowski, B.F., Butler, B.L., Stecha, P.F., Eggers, C.T., Otto, P., Zimmerman, K., Vidugiris, G., Wood, M.G., Encell, L.P., Fan, F., and Wood, K.V. (2011). A luminescent biosensor with increased dynamic range for intracellular cAMP. ACS Chem Biol *6*, 1193-1197. 10.1021/cb200248h.
49. Zhu, Z., Di, J., Lu, Z., Gao, K., and Zheng, J. (2016). Rap2B GTPase: structure, functions, and regulation. Tumour Biol *37*, 7085-7093. 10.1007/s13277-016-5033-y.
50. Benjamin J. Polacco, B.T.L., Emily E. Blythe, Nohely Abreu, Prachi Khare, Matthew K. Howard, Alberto J. Gonzalez-Hernandez, Jiewei Xu, Qiongyu Li, Brandon Novy, Zun Zar Chi Naing, Brian K. Shoichet, Willow Coyote-Maestas, Joshua Levitz, Nevan J. Krogan, Mark Von Zastrow & Ruth Hüttenhain (2024). Profiling the proximal proteome of the activated μ-opioid receptor.
51. Kushner, J., Papa, A., and Marx, S.O. (2021). Use of Proximity Labeling in Cardiovascular Research. JACC Basic Transl Sci *6*, 598-609. 10.1016/j.jacbts.2021.01.005.
52. Godin, P., Tsoi, M.F., Morin, M., Gevry, N., and Boerboom, D. (2022). The granulosa cell response to luteinizing hormone is partly mediated by YAP1-dependent induction of amphiregulin. Cell Commun Signal *20*, 72. 10.1186/s12964-022-00843-1.
53. Ohbayashi, N., Fukuda, M., and Kanaho, Y. (2017). Rab32 subfamily small GTPases: pleiotropic Rabs in endosomal trafficking. J Biochem *162*, 65-71. 10.1093/jb/mvx027.
54. Bultema, J.J., Ambrosio, A.L., Burek, C.L., and Di Pietro, S.M. (2012). BLOC-2, AP-3, and AP-1 proteins function in concert with Rab38 and Rab32 proteins to mediate protein trafficking to lysosome-related organelles. J Biol Chem *287*, 19550-19563. 10.1074/jbc.M112.351908.

55. Keiper, M., Stope, M.B., Szatkowski, D., Bohm, A., Tysack, K., Vom Dorp, F., Saur, O., Oude Weernink, P.A., Evellin, S., Jakobs, K.H., and Schmidt, M. (2004). Epac- and Ca2+ -controlled activation of Ras and extracellular signal-regulated kinases by Gs-coupled receptors. J Biol Chem *279*, 46497-46508. 10.1074/jbc.M403604200.